Enhanced Artificial Coronary Circulation System Algorithm for Truss Optimization with Multiple Natural Frequency Constraints

Ali Kaveh[1*], Mohsen Kooshkbaghi[2]

[1] Department of Civil Engineering,
  Iran University of Science and Technology,
  Narmak, Postal Code 1684613114, Tehran, Iran
[2] Department of Civil Engineering,
  Science and Research Branch,
  Islamic Azad University, Tehran, Iran
* Corresponding author, e-mail: alikaveh@iust.ac.ir

Abstract

In this paper, an enhanced artificial coronary circulation system (EACCS) algorithm is applied to structural optimization with continuous design variables and frequency constraints. The standard algorithm, artificial coronary circulation system (ACCS), is inspired biologically as a non-gradient algorithm and mimics the growth of coronary tree of heart circulation system. Designs generated by the EACCS algorithm are compared with other popular evolutionary optimization methods, the objective function being the total weight of the structures.

Truss optimization with frequency constraints has attracted substantial attention to improve the dynamic performance of structures. This kind of problems is believed to represent nonlinear and non-convex search spaces with several local optima. These problems are also suitable for examining the capabilities of the new algorithms. Here, ACCS is enhanced (EACCS) and employed for size and shape optimization of truss structures and six truss design problems are utilized for evaluating and validating of the EACCS. This algorithm uses a fitness-based weighted mean in the bifurcation phase and runner phase of the optimization process. The numerical results demonstrate successful performance, efficiency and robustness of the new method and its competitive performance to some other well-known meta-heuristics in structural optimization.

Keywords

meta-heuristic, ACCS algorithm, enhanced ACCS algorithm, structural optimization, shape and size optimization, frequency constraints

1 Introduction

Optimal design of truss structures subjected to dynamic behavior has been a challenging area of study and it is an active research area. Optimal truss design subjected to frequency bounds is a valuable tool for improving the dynamic behavior of the truss [1–5]. Natural frequencies of a truss should be enforced to avoid resonance with an external excitation. In addition, engineering compositions should be as light as possible. On the other hand, mass minimization conflicts with frequency bounds and increases the complexity of the problem [6, 8, 9]. As such, an expeditious optimization method is required to design the trusses susceptible to fundamental frequency constraints, and continuous effort is put by researchers in this aspect [7, 10].

Size, shape, and topology optimizations are three main kinds of truss optimization. In size optimization, the final goal is to acquire the best bar sections, whereas shape optimization insures the best nodal positions of predefined nodes of the truss structure. The effect of shape and sizing on objective function and constraints are in conflict. Hence, simultaneous shape and sizing optimization with natural frequency bounds adds further complexity and often leads to fluctuations [11]. Several researchers have been using different optimization algorithms, yet this research area has not yet been fully investigated. In recent years, many optimization techniques have been studied in this application area [12–17].

Structural optimization can be categorized into two classes: discrete structural optimization and continuum structural optimization. Discrete structural optimization is also best-known as truss optimization, having connectivity of finite dimension parameters as variables (naturally discrete parameter system) and continuum structural optimization have field as a variable (discretized parameter system) [18–20].

This paper suggests the application of the recently developed optimization algorithm, so-called the Artificial Coronary Circulation System (ACCS) [21], for optimum design of truss structures with frequency constraints. Moreover, an enhanced version of the ACCS, called EACCS, is applied to the problem in hand. In this method, the solution candidates are considered as capillaries leaders that growth in direction best position for enhancing the dissemination system. Improving heart circulation system is achieved from current population and historically best position in order to have a suitable balance between exploration and exploitation.

In order to evaluate the performance of the ACCS, six truss structures are optimized for minimum weight with the design variables being considered as the cross-sectional areas of the members and/or the coordinates of some nodes. The truss examples have 10, 72, 120, 200, 37 and 52 members, respectively. The numerical results indicate that the planned algorithm is rather competitive with other state-of-the-art metaheuristic methods.

This study has been organized as follows: In Sect. 2, the mathematical formulation of the structural optimization with frequency constraints is stated. The enhanced algorithm EACCS is presented after a brief overview of the standard ACCS in Sect. 3. Six structural design examples are studied in Sect. 4, and some concluding remarks are eventually provided in Sect. 5.

2 Statement of the optimization problem

In a frequency constraint truss shape and size optimization problem, the goal is to minimize the weight of the structure while satisfying some constraints on natural frequencies. The design variables are the cross-sectional areas of the members and/or the coordinates of some nodes. The topology of the structure is not expected to be changed and thus the connectivity of the structure is predefined and kept unaltered during the optimization process. For each one of the design variables should be chosen from a permissible range. The optimization problem can be stated mathematically as follows:

$$Find \ X = [x_1, x_2, \ldots, x_n], \tag{1}$$

$$To \ minimizes \quad G(X) = f(X) \cdot (1 + f_{penalty}(X))$$

$$Subjected \ to \begin{cases} \omega_j \leq \omega_j^* & for \ some \ natural \ frequencies \ j \\ \omega_k \geq \omega_k^* & for \ some \ natural \ frequencies \ k \end{cases} \tag{2}$$

$$x_{min} \leq x_i \leq x_{max},$$

where X is the vector of the design variables, including both nodal coordinates and cross-sectional areas. Here, n is the number of variables which is naturally affected by the element grouping scheme which in turn is chosen considering the symmetry and practice requirements. $G(X)$ is the merit function; $f(X)$ is the cost function, which has been taken as the weight of the structure in a weight optimization problem; $f_{penalty}(X)$ is the penalty function that is used to make the problem unconstrained. When all of the constraints are contented, the penalty function value is equal to unity; ω_j is the jth natural frequency of the structure and ω_j^* is its upper bound. ω_k is the kth natural frequency of the structure and ω_k^* is its lower bound; x_{min} and x_{max} are the lower and upper bounds of the design variable x_i, respectively. The cost function is expressed as:

$$f(X) = \sum_{i=1}^{N_{var}} \rho_i L_i A_i, \tag{3}$$

where ρ_i is the material density of member i; L_i is the length of member i; and A_i is the cross-sectional area of the ith member.

The penalty function is defined as:

$$f_{penalty}(X) = (1 + \varepsilon_1 . c)^{\varepsilon_2} \quad c = \sum_{i=1}^{q} c_i, \tag{4}$$

where q is the number of frequency constraints. If the ith constraint is satisfied, c_i will be taken as zero, otherwise it will be considered as:

$$c_i = \begin{cases} 0 & if \ the \ ith \ constraint \ is \ satisfied \\ \left| 1 - \dfrac{\omega_i}{\omega_i^*} \right| & else \end{cases} \tag{5}$$

The parameters and are selected considering the exploration and the exploitation rate of the search space. In this study is taken as unity, and starts from 1.5 and linearly increases to 6 in all the test examples. These values penalize the unfeasible solutions more severely as the optimization procedure proceeds. As a result, in the primal stages, the agents are autonomous to explore the search space, but at the end they tend to choose solutions without violation.

3 Artificial Coronary Circulation System (ACCS) Optimization

ACCS is a coronary tree growth process inspired algorithm, proposed by Kaveh and Kooshkbaghi [21]. This algorithm is based on coronary circulation of the heart muscle. The ACCS algorithm consists of two basic modes of the growing coronary tree: (i) produce stem-crown (known as bifurcation phase), and (ii) growing with the other capillaries (known as pruning phase). In this optimization algorithm an initial group of capillaries is considered as population and different main arteries are considered as different design variables of the optimization problem and a capillary leader's result is analogous to the "fitness value" of the optimization problem. In this algorithm, any branches of coronary tree is considered as a new solution and the total cost of the tree at any end is considered as the cost of the object function at any solution. With these values, the Coronary Growth Factor (CGF) is calculated for any solution. This result is analogous to the fitness value of the optimization problem. Also, the best solution in the entire population is considered as the stem, and the best solution is the minimum value of the CGF.

The process of the ACCS is divided into two main parts, 'Bifurcation phase' and 'Pruning phase'. The ACCS procedure can be briefly outlined as follows:

3.1 Bifurcation and Pruning phase (Global Search)

During this phase, a capillary leader tries to improve the CGF of the center of the suggested capillary leaders by the end of stem. Thus, at any iteration t, it is assumed that there are N_{var} number of main arteries (i.e. design variables, $j = 1, 2, \ldots, N_{var}$), Npop is the number of capillary leaders (i.e. population size, $i = 1, 2, \ldots, N_{pop}$) and $X_c^{t,j}$ is the mean of all the jth subjects of capillary leaders in a current capillaries population. However, the best capillary leader (CL) identified is considered by the algorithm as the stem. Thus, the CGF of the CLs are mathematically formulated as follows:

$$CGF_i^t = \frac{1/fit_i}{\sum 1/fit_i}, \quad i = 1, 2, \ldots, N_{pop},$$ (6)

$$CGF_c^t = \frac{1/fit_c}{\sum 1/fit_i},$$ (7)

$$fit_c = mean(fit_i).$$ (8)

Then the existing solution is updated in the bifurcation phase according to the following expression:

$$X_{i,j}^{t+1} = X_{i,j}^t + dir.B_f.\left(X_{c,j}^t - rand.X_{i,j}^t\right)$$
$$i = 1, \&, N_{pop}, \quad j = 1, \&, N_{var},$$ (9)

$$\begin{cases} dir = -1 & if \quad CGF_c^t < CGF_i^t \\ dir = +1 & else \end{cases},$$ (10)

$$X_{c,j} = mean\left(X_j^t\right) \quad j = 1, \ldots, N_{var},$$ (11)

where $X_{i,j}^{t+1}$ indicates the new position value of the jth variable for the ith CL; and "dir" denotes the growth direction; and "$rand$" is a random number uniformly distributed in the range of (0,1); B_f is the bifurcation factor and it determines the growth step and is equal to CGF_i; and $X_{i,j}^t$ indicates the old position value of the jth variable for the ith CL.

3.2 Runner and Pruning phase (Local Search)

As mentioned in the previous steps, the best CLs are considered as the main arteries leaders and are converted to stems and the coronary tree grows. In this stage, all the new CLs grow at the end of the stems and create new CLs. Also, the CLs growth is based on the coronary growth factor (CGF) of the arteries leader along the coronary arteries tree. Therefore, an exponent factor is defined as follow:

$$X_{i,j}^{t+1} = X_{i,j}^t + \alpha.rand.\left(X_{b,j}^t - X_{w,j}^t\right),$$ (12)

where $X_{i,j}^{t+1}$ determines the new position value of the jth variable for the ith CL; and $X_{i,j}^t$ determines the old position value of the jth variable for the ith CL; α is angiogenesis index and it is a decreasing function of time, which controls the pumping power of the heart. It is initialized to 1 at the beginning of the algorithm and is exponentially decreased to about 0.6 as the iterations elapse; and $rand$ is a random numbers uniformly distributed in the range of (0,1); and $X_{b,j}^t$ and $X_{w,j}^t$ are the best and the worst CLs of the last (old) population which refer to the best arteries leader and the worst arteries leader. According to the above equations, each CL searches the space for the new position for growth as the capillaries.

Therefore, after each above mechanism, the best and worst CLs are found and the old values are updated. Also any component of the solution vector violating the variable boundaries can be regenerated from the Heart Memory (HM). Then, a memory is considered which saves the best CL vectors and their related coronary growth factor (CGF) values. So, the Heart Memory Considering Rate (HMCR) varying between 0 and 1 sets the rate of choosing a value

in the new values from the historic values stored in the HM. In this study, the size of the HM (i.e. HMS) is taken as 5 and the HMCR is considered as 0.95.

3.3 Enhanced Artificial Coronary Circulation System

The purpose of this section is to introduce an improved version of the standard ACCS, Enhanced Artificial Coronary Circulation System (EACCS) optimization modifies the ACCS to get better solutions. The ACCS and EACCS use a heart memory (HM) for saving some of the best solutions and updating them in each iteration. The HM enables the ACCS and EACCS to have a stronger exploitation and better convergence. Furthermore, using a mechanism to change some components of capillaries leaders helps the algorithm to escape from local optima. The EACCS procedure is similar to that of ACCS, where only one step is added to its procedure:

Step 1: *Initialization*

The initial positions for CLs are determined randomly in the search space as:

$$X_i^0 = X_{min} + rand.\left(X_{max} - X_{min}\right), \quad i = 1,\ldots,n_{pop}, \qquad (13)$$

where $X_{i,j}^0$ is the initial solution vector of the *i*th CL. Here, X_{min} and X_{max} are the bounds of design variables; *rand* is a random vector with each component being in the interval [0,1]; N_{pop} is the number of the population of CLs.

Step 2: *Defining Coronary Growth Factor (CGF)*

The value of CGF for each CL is evaluated according to Eqs. (6 and 7).

Step 3: *Storing*. Heart memory (HM) is utilized to save several historically best capillary leaders (CL vectors) and their related CGF and the objective function values. Solution vectors that are saved in the HM are added to the population, and the same number of current worst CLs is deleted. Finally, CLs are sorted according to their objective function values in an increasing order. Using this mechanism can improve the algorithm performance without increasing the computational cost.

Step 4: *Bifurcation and Pruning phase and Jump out*: To improve the exploration capability of the standard ACCS and to prevent premature convergence, a stochastic approach is used in EACCS. A parameter like *Pro* that is a number within (0,1) is introduced and specified whether a component of each CL must be changed or not. The value of *Pro* is evaluated according to Eq. (14).

$$\boldsymbol{Pro} = \omega_{min} + \left(\frac{itr}{itr_{max}}\left(\omega_{max} - \omega_{min}\right)\right) \qquad (14)$$

In this paper, the value of *Pro* is equal to 0.1 at the beginning of the search to emphasize the exploration, and then it is linearly increased to 0.3 at the end to encourage the exploitation.

For each CL, *Pro* is compared with $\boldsymbol{Rand}_i$ ($i = 1,\ldots,N_{pop}$), which is a random number uniformly distributed within (0, 1). Thus, the design variable of the *i*th CL value is regenerated by

$$\begin{cases} Eqs.(9) \ and \ (10) \ and \ (16) & if \ Rand_i < Pro \\ X_{i,j} = X_{min,j} + rand.\left(X_{max,j} - X_{min,j}\right) & else \end{cases}, (15)$$

$$X_{c,j} = \frac{\sum_{i=1}^{n_{pop}} \dfrac{X_j}{fit_i}}{\sum_{i=1}^{n_{pop}} \dfrac{1}{fit_i}} \quad j = 1,\ldots,n_{var}, \qquad (16)$$

where $X_{i,j}$ = *j*th design variable of the *i*th CL; $X_{min,j}$ and $X_{max,j}$ are minimum and maximum limits of the *j*th design variable. Then, the CLs are updated and sorted according to their objective function values.

Step 5: *Runner and Pruning phase*. Updating CLs and the new position of each CL are performed by Eq. (12). The updated CLs are sorted according to their objective function values.

Step 6: *Updating Heart Memory*. Keeping the best CLs in each iteration.

Step 7: *Terminating condition check*. The process of optimization is terminated after the predefined maximum evaluation number. Otherwise, the process is continued by going to Step 2.

A flowchart of the EACCS algorithm is shown in Fig. 1.

4 Numerical examples

In this section, six most often used numerical examples are studied by the proposed methods. These examples consist of four truss structures for size optimization and two structures for shape and size optimization. The performance of the standard ACCS and EACCS are examined through six standard design optimization problems.

These examples include some well-known planar and space trusses. The population number of the CLs or agents for these examples is taken as 20 for both methods. Also, for all these examples the maximum number of iterations is considered as 200. Material properties, cross-sectional area bounds, and frequency constraints are provided in Table 1.
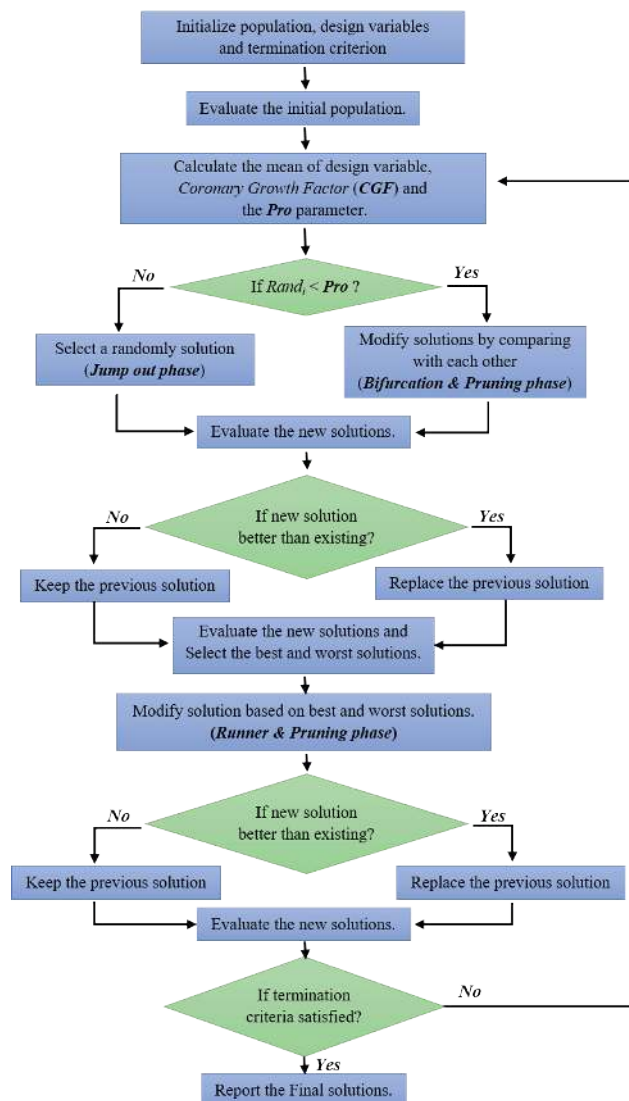
Fig. 1 A Flowchart Of The EACCS Algorithm

Table 1 Material properties, cross-sectional area bounds, and frequency constraints for different problems.

Problem	Property (unit)			
	Young's modulus (N/m²)	Material density (kg/m³)	Cross-sectional area bounds (cm²)	Frequency constraints (Hz)
10-bar planar truss	6.89×10^{10}	2770	$0.645 \times 10^{-4} \leq A_i$	$f_1 \geq 7$ $f_2 \geq 15$ $f_3 \geq 20$
72-bar space truss	6.89×10^{10}	2770	$0.645 \times 10^{-4} \leq A_i$	$f_1 = 4$ $f_2 \geq 6$
120-bar dome truss	2.1×10^{11}	7971.81	$0.0001 \leq A_i \leq 0.01293$	$f_1 \geq 9$ $f_2 \geq 11$
200-bar planar truss	2.1×10^{11}	7860	$0.1 \times 10^{-4} \leq A_i$	$f_1 \geq 5$ $f_2 \geq 10$ $f_3 \geq 15$
37-bar planar truss	2.1×10^{11}	7800	$0.1 \times 10^{-4} \leq A_i$	$f_1 \geq 20$ $f_2 \geq 40$ $f_3 \geq 60$
52-bar dome truss	2.1×10^{11}	7800	$0.0001 \leq A_i \leq 0.001$	$f_1 \leq 15.9155$ $f_2 \geq 28.6479$
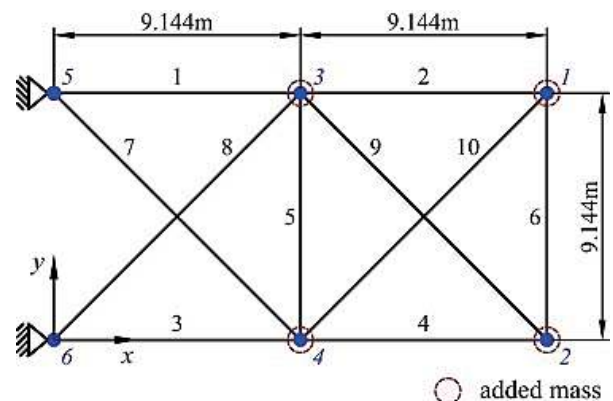
Fig. 2 Schematic of a 10-bar planar truss structure

For all examples, 10 independent optimization runs are executed as meta-heuristic algorithms have stochastic nature and their performance may be sensitive to initial population. The frequency constraints are handled using the well-known penalty approach.

Subsequently, statistical results are presented in terms of the best weight and the corresponding number of FE analyses, the mean weight and standard deviation. Only design variable values achieved from the best run are reported for comparison with those given by other optimization approaches to illustrate the accuracy and robustness of the proposed algorithm. Also, the ACCS and EACCS algorithms and the direct stiffness method for the analysis of truss structures are coded in MATLAB software. The example results are based on a Laptop with a CPU 2.4 GHz, and 6.0 GB of RAM. Also, the operation system is Windows 10 and the version of the MATLAB is R2016a.

4.1. Size optimization
4.1.1 The 10-bar plane truss
Schematic of the 10-bar plane truss, displayed in Fig. 2, is the first test problem. The cross-sectional area of each of the members is an independent variable. Here, cross-sectional areas of all bars are treated as continuous design variables. Four nonstructural masses of 454 kg are assigned with four free nodes as indicated in the same figure. Besides, as one of the benchmark problems, this structure has been studied by other researchers that are listed in the pursuing literature [4–6, 8–10, 17, 22–24].

Table 2 shows a comparison of the optimal results obtained by the present algorithms with different approaches. The optimal weight accomplished by the proposed EACCS is

Table 2 Comparison of optimal results of the 10-bar planar truss obtained by different algorithms

| Design variable (cm$_2$) | GA [22] | PSO [5] | CSS [8] | FA [10] | This work | |
					ACCS	EACCS
A_1	42.230	37.712	38.811	36.198	35.5557	35.0354
A_2	18.555	09.959	09.0307	14.030	15.1448	15.0132
A_3	38.851	40.265	37.099	34.754	35.4367	35.4505
A_4	11.222	16.788	18.479	14.900	14.8101	15.0603
A_5	04.783	11.576	04.479	00.654	0.651	0.6475
A_6	04.451	03.955	04.205	04.672	4.5225	4.5224
A_7	21.049	25.308	20.842	23.467	23.9125	23.4493
A_8	20.949	21.613	23.023	25.508	23.1290	23.4182
A_9	10.257	11.576	13.763	12.707	12.0245	12.1051
A_{10}	14.342	11.186	11.414	12.351	12.3559	12.7158
Best weight (kg)	542.750	537.980	531.950	531.280	524.6371	524.6001
Average weight (kg)	552.447	540.890	536.390	535.070	525.4842	525.0068
Standard deviation	04.864	06.840	03.320	03.640	2.8756	0.3030
No. of analyses	13,777	20,000	4,000	5,000	8,000	8,000

Note: GA = Genetic Algorithm; PSO = particle swarm optimization; CSS = charged system search; FA = firefly algorithm; CPA= Cyclical Parthenogenesis Algorithm; ACCS = Artificial Coronary Circulation System; N/A = not available.

Table 3 Natural frequencies (Hz) of the optimized designs for the 10-bar planar truss

| Frequency no. | GA [22] | PSO [5] | CSS [8] | FA [10] | This work | |
					ACCS	EACCS
1	07.008	07.000	07.000	07.0002	07.0000	07.0000
2	18.148	17.786	17.442	16.1640	16.2358	16.2094
3	20.000	20.000	20.031	20.0029	20.0000	20.0000
4	20.508	20.063	20.208	20.0221	20.0018	20.0001
5	27.797	27.776	28.261	28.5428	28.3855	28.4486
6	31.281	30.939	31.139	28.9220	28.8872	29.0761
7	48.304	47.297	47.704	48.3538	48.8085	48.7494
8	53.306	52.286	52.420	50.8004	51.2694	51.2833

better than other methods. Table 3 represents the first eight optimal natural frequencies obtained by the present work and different researches. All the frequencies strictly satisfy the allowable constraints and no constraint is violated.

The best and average convergence curves for these algorithms are illustrated in Fig. 3. This algorithm rapidly discovers the optimal solution with only 5860 analyses, while the others algorithms require a larger number of analyses for the convergence. Also, the EACCS has minimum standard deviation among the presented solutions.

4.1.2 The 72-bar space truss
The second example aims to optimize a 72-bar space truss whose geometry and finite element model are depicted in Fig. 4. The values of the cross-sectional area, minimum weight, and statistical information of the solution obtained

by the standard ACCS, EACCS, and some other previous studies reported in the literature are presented in Table 4. Four non-structural masses of 2270 kg are attached to four upper nodes. This is also a benchmark problem that has previously been examined by a variety of researchers such as Refs. [6, 8, 9, 17].

Optimal results obtained by the present methods with different algorithms are provided in Table 4 for comparison. As it can be observed, the EACCS results in the smallest weight in comparison to the other algorithms. Table 5 reports the natural frequencies of the optimized structures; clearly, none of the frequency constraints are violated. The weight convergence histories obtained using both algorithms for this example are illustrated in Fig. 5. It is found that the EACCS needs far fewer number of FE analyses to gain the optimal solution compared to the other algorithms.

**Table 4** Optimal cross-sectional areas for the 72-bar space truss (cm²)

Group No.	Elements	PSO [5]	HS [10]	CSS [8]	FA [10]	CPA [6]	This work	
							ACCS	EACCS
G_1	1–4	2.987	3.6803	2.528	3.341	3.329	4.1886	3.7122
G_2	5–12	7.849	7.6808	8.704	7.759	7.841	7.9958	7.7434
G_3	13–16	0.645	0.6450	0.645	0.645	0.645	0.6813	0.6468
G_4	17–18	0.645	0.6450	0.645	0.645	0.645	0.7430	0.697
G_5	19–22	8.765	9.4955	8.283	9.020	8.416	6.4211	8.2884
G_6	23–30	8.153	8.2870	7.888	8.257	8.160	7.6720	8.2141
G_7	31–34	0.645	0.6450	0.645	0.645	0.645	0.7656	0.6658
G_8	35–36	0.645	0.6461	0.645	0.645	0.645	0.7014	0.6743
G_9	37–40	13.450	11.4510	14.666	12.045	13.078	14.0034	12.15
G_{10}	41–48	8.073	7.8990	6.793	8.040	8.043	8.1338	7.87
G_{11}	49–52	0.645	0.6473	0.645	0.645	0.645	0.6612	0.7058
G_{12}	53–54	0.645	0.6450	0.645	0.645	0.645	0.6810	0.6526
G_{13}	55–58	16.684	17.4060	16.464	17.380	16.943	17.1666	17.0882
G_{14}	59–66	8.159	8.2736	8.809	8.056	8.143	7.9807	7.9472
G_{15}	67–70	0.645	0.6450	0.645	0.645	0.647	0.7097	0.645
G_{16}	71–72	0.645	0.6450	0.645	0.645	0.653	0.6532	0.7462
Best weight (kg)	328.823	328.334	328.814	327.690	328.490	326.7081	325.1956	
Average weight (kg)	-	332.640	337.700	329.890	330.910	327.9035	326.3036	
Standard deviation	-	2.390	5.420	2.590	1.840	1.3413	0.650	
No. of analyses	-	50,000	4,000	10,000	12,800	12,000	12,000	
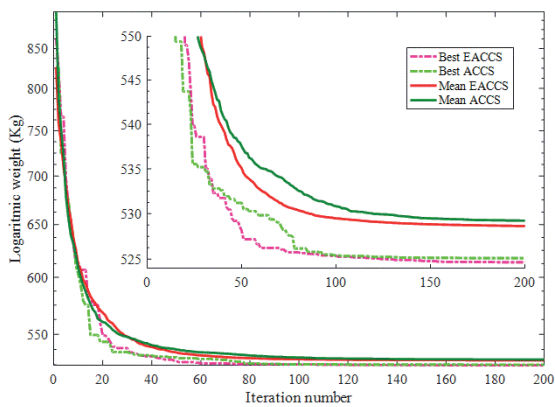
Fig. 3 The weight convergence histories of the 10-bar planar truss obtained using the ACCS and EACCS

4.1.3 The 120-bar dome truss

The third example aims to optimize a 120-bar dome truss as shown in Fig. 6. Non-structural masses are attached to all the free nodes as follows: 3,000 kg at Node 1, 500 kg at Nodes 2–13, and 100 kg at the remaining nodes. The symmetry of the structure about the x-axis and y-axis is considered to group the 120 members into seven independent size variables. This is also a benchmark problem that has been previously examined in a variety of studies such as [7–9, 17, 25].
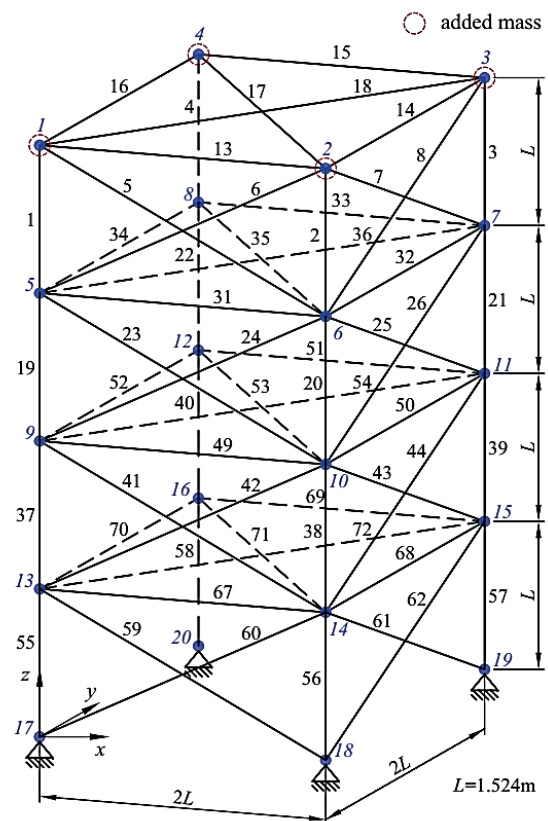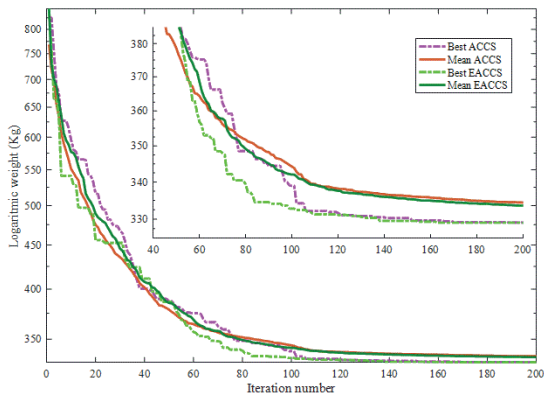

Fig. 4 The 72-bar space truss

Fig. 5 The weight convergence histories of the 72-bar planar truss obtained using the ACCS and EACCS

Table 6 presents a comparison of the optimal results obtained by this work with those available in the literature. It can be noticed that in this case, the EACCS has the smallest optimal weight compared to the others. As reveals from the table, the standard deviation of the EACCS is lower than the others. The optimized structural frequencies (Hz) for these methods are presented in Table 7. None of the frequency constraints are violated. Fig. 7 shows the weight convergence histories obtained using both ACCS and EACCS algorithms for this problem.
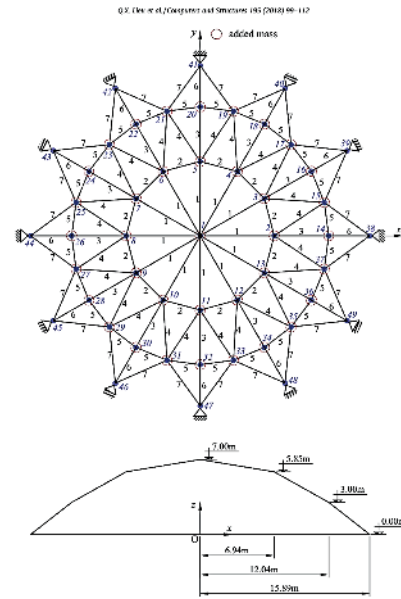

Fig. 6 The 120-bar dome truss

Table 5 Natural frequencies (Hz) of the optimized designs for the 72-bar planar truss

Frequency No.	PSO [5]	HS [10]	CSS [8]	FA [10]	CPA [6]	This work	
						ACCS	EACCS
1	4.000	4.0000	4.000	4.000	4.000	4.0000	4.0000
2	4.000	4.0000	4.000	4.000	4.000	4.0000	4.0000
3	6.000	6.0000	6.006	6.000	6.000	6.0112	6.0007
4	6.219	6.2723	6.210	6.247	6.238	7.6655	6.4325
5	8.976	9.0749	8.684	9.038	9.035	9.7585	9.1635

Table 6 Comparison of optimal results of the 120-bar dome truss obtained by different algorithms

Design variable A_i (cm²)	CSS [8]	CBO [26]	PSO [7]	VPS [13]	SOS [17]	This work	
						ACCS	EACCS
A_1	21.710	19.6917	23.494	19.6836	19.5203	19.3331	19.5342
A_2	40.862	41.1421	32.976	40.9581	40.8482	40.9855	40.3209
A_3	09.048	11.1550	11.492	11.3325	10.3225	10.4487	10.5741
A_4	19.673	21.3207	24.839	21.5387	20.9277	20.9748	21.0753
A_5	08.336	09.8330	09.964	09.8867	09.6554	9.80400	09.7126
A_6	16.120	12.8520	12.039	12.7116	12.1127	12.0105	11.7997
A_7	18.976	15.1602	14.249	14.9330	15.0313	14.8797	14.9179
Best weight (kg)	9204.510	8889.1303	9171.93	8888.74	8713.3030	8704.7655	8703.7014
Average weight (kg)	-	8891.2540	9251.84	8896.04	8735.3452	8728.0188	8704.4643
Standard deviation	-	1.7926	89.380	6.650	17.9011	12.2037	0.7839
No. of analyses	4,000	6,000	6,000	30,000	4,000	8,000	6,000

Table 7 Natural frequencies (Hz) of the optimized designs for the 120-bar planar truss

Frequency No.	CSS [8]	CBO [26]	PSO [7]	VPS [13]	SOS [17]	This work	
						ACCS	EACCS
1	09.002	09.0000	09.0000	09.0000	09.0009	09.0000	09.0000
2	11.002	11.0000	11.0000	11.0000	11.0005	11.0000	11.0000
3	11.006	11.0000	11.0052	11.0000	11.0005	11.0026	11.0027
4	11.015	11.0096	11.0134	11.0096	11.0046	11.0112	11.0113
5	11.045	11.0494	11.0428	11.0491	11.0714	11.0685	11.0682

Fig. 7 The weight convergence histories of the 120-bar planar truss obtained using the ACCS and EACCS

4.1.4 The 200-bar planar truss

A planar truss containing 200 bars, shown in Fig. 8, is optimized as the last example of the type of size optimization problem of truss structures with multiple frequency constraints. At upper nodes of the structure, non-structural masses of 100 kg are added for the free vibration analysis. Members of the structure are categorized into 29 groups corresponding to 29 design variables as indicated in Table 8. This example has formerly been considered in detail by numerous researchers with different methods [6–9].

Similar to the previously illustrated examples, optimal results obtained by the present algorithms and different approaches are summarized in Table 8 for comparison. As it can be seen, the best and average weight and standard deviation corresponding to the EACCS are better than some of the other methods. Furthermore, the number of FE analyses used to gain the optimal weight is the least for the EACCS.

Optimal natural frequencies obtained by different algorithms are displayed in Table 9. It can be recognized that none of the constraints are violated. The weight convergence histories obtained using both algorithms for this structure are shown in Fig. 9. Clearly, the convergence rate of the EACCS is always better than the other algorithms.

Fig. 8 The 200-bar planar truss

Fig. 9 The weight convergence histories of the 200-bar planar truss obtained using the ACCS and EACCS

Table 8 Optimal cross-sectional areas for the 200-bar planar truss (cm^2)

Ai (cm²)	Member group	CSS [8]	TLBO [28]	SOS [17]	This work ACCS	This work EACCS
	Design variable					
1	1, 2, 3, 4	0.2439	0.3030	0.4781	0.3262	0.3175
2	5, 8, 11, 14, 17	0.1438	0.4479	0.4481	0.406	0.4452
3	19, 20, 21, 22, 23, 24	0.3769	0.1001	0.1049	0.1062	0.1004
4	18, 25, 56, 63, 94, 101, 132, 139, 170, 177	0.1494	0.1000	0.1045	0.1082	0.1004
5	26, 29, 32, 35, 38	0.4835	0.5124	0.4875	0.4917	0.4964
6	6, 7, 9, 10, 12, 13, 15, 16, 27, 28, 30, 31, 33, 34, 36, 37	0.8103	0.8205	0.9353	0.8509	0.8226
7	39, 40, 41, 42	0.4364	0.1000	0.1200	0.1024	0.1095
8	43, 46, 49, 52, 55	1.4554	1.4499	1.3236	1.4816	1.3878
9	57, 58, 59, 60, 61, 62	1.0103	0.1001	0.1015	0.1318	0.1006
10	64, 67, 70, 73, 76	2.1382	1.5955	1.4827	1.6093	1.5465
11	44, 45, 47, 48, 50, 51, 53, 54, 65, 66, 68, 69, 71, 72, 74, 75	0.8583	1.1556	1.1384	1.1354	1.1541
12	77, 78, 79, 80	1.2718	0.1242	0.1020	0.1196	0.1592
13	81, 84, 87, 90, 93	3.0807	2.9753	2.9943	3.0434	2.9979
14	95,96, 97, 98, 99, 100	0.2677	0.1000	0.1562	0.3132	0.1007
15	102, 105, 108, 111, 114	4.2403	3.2553	3.4330	3.2862	3.2726
16	82, 83, 85, 86, 88, 89, 91, 92, 103, 104, 106, 107, 109, 110, 112, 113	2.0098	1.5762	1.6816	1.5869	1.5753
17	115, 116, 117, 118	1.5956	0.2680	0.1026	0.2249	0.2768
18	119, 122, 125, 128, 131	6.2338	5.0692	5.0739	5.085	5.0434
19	133, 134, 135, 136, 137, 138	2.5793	0.1000	0.1068	0.1709	0.1076
20	140, 143, 146, 149, 152	3.0520	5.4281	6.0176	5.2071	5.449
21	120, 121, 123, 124, 126, 127, 129, 130, 141, 142, 144, 145, 147, 148,150, 151	1.8121	2.0942	2.0340	2.2289	2.1447
22	153, 154, 155, 156	1.2986	0.6985	0.6595	0.2708	0.6745
23	157, 160, 163, 166, 169	5.8810	7.6663	6.9003	8.027	7.6967
24	171, 172, 173, 174, 175, 176	0.2324	0.1008	0.2020	0.2105	0.1353
25	178, 181, 184, 187, 190	7.7536	7.9899	6.8356	7.8354	7.7106
26	158, 159, 161, 162, 164, 165, 167,168, 179, 180, 182, 183, 185, 186, 188, 189	2.6871	2.8084	2.6644	2.9012	2.7915
27	191, 192, 193, 194	12.5094	10.4661	12.1430	9.5438	10.3755
28	195, 197, 198, 200	29.5704	21.2466	22.2484	21.438	21.3364
29	196, 199	8.2910	10.7340	8.9378	11.307	10.7345
Best weight (kg)		2259.86	2156.541	2180.3210	2167.4954	2156.3651
Average weight (kg)		-	2157.547	2303.3034	2180.3886	2157.6554
Standard deviation		-	1.545	83.5897	8.1411	1.7683
No. of analyses		10,000	23,000	10,000	23,000	23,000

Table 9 Natural frequencies (Hz) of the optimized designs for the 200-bar planar truss

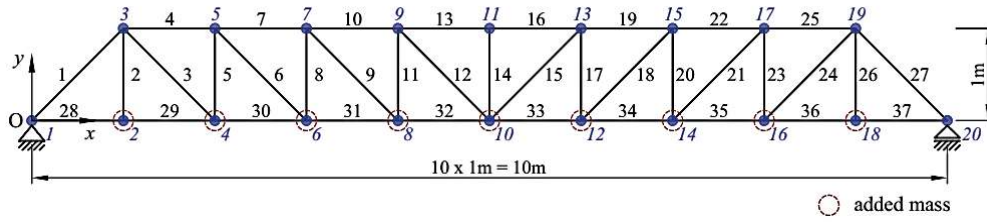| Frequency No.	CSS [8]	TLBO [28]	SOS [17]	This work ACCS	This work EACCS
1	5.010	5.00000	5.0001	5.0000	5.0000
2	12.911	12.21710	13.4306	12.3550	12.3137
3	15.416	15.03796	15.2645	15.0212	15.0226
4	17.033	16.70476	-	16.8172	16.6997
5	21.426	21.40164	-	21.4369	21.4152
6	21.613	21.45347	-	21.7894	21.6432

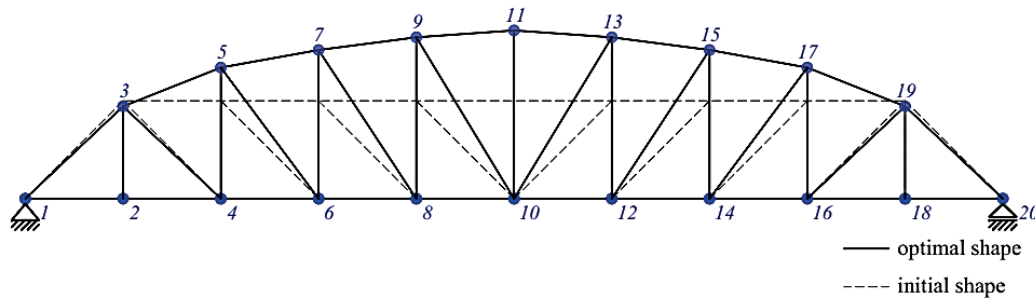Fig. 10 The initial shape of the 37-bar planar truss

Fig. 11 Final configuration found by the artificial coronary circulation system algorithm for the simply supported planar 37-bar truss

Table 10 Comparison of optimal results of the 37-bar planar truss obtained by different algorithms

Design variable Y_j (m) ; A_i (cm²)	Initial	PSO [5]	HS [10]	CSS [8]	SOS [17]	This work	
						ACCS	EACCS
Y3; Y19	1.0000	0.9637	0.8415	0.8726	0.9598	0.9958	0.9352
Y5; Y17	1.0000	1.3978	1.2409	1.2129	1.3867	1.405	1.3114
Y7; Y15	1.0000	1.5929	1.4464	1.3826	1.5698	1.5976	1.4983
Y9; Y13	1.0000	1.8812	1.5334	1.4706	1.6687	1.7117	1.6284
Y11	1.0000	2.0856	1.5971	1.5683	1.7203	1.818	1.7064
A1; A27	1.0000	2.6797	3.2031	2.9082	2.9038	2.8671	2.9045
A2; A26	1.0000	1.1568	1.1107	1.0212	1.0163	1.0717	1.0013
A3; A24	1.0000	2.3476	1.1871	1.0363	1.0033	1.0035	1.0156
A4; A25	1.0000	1.7182	3.3281	3.9147	3.1940	2.2862	2.6157
A5; A23	1.0000	1.2751	1.4057	1.0025	1.0109	1.3468	1.1372
A6; A21	1.0000	1.4819	1.0883	1.2167	1.5877	1.1864	1.2058
A7; A22	1.0000	4.6850	2.1881	2.7146	2.4104	2.415	2.5863
A8; A20	1.0000	1.1246	1.2223	1.2663	1.3864	1.5053	1.3730
A9; A18	1.0000	2.1214	1.7033	1.8006	1.6276	1.3932	1.4763
A10; A19	1.0000	3.8600	3.1885	4.0274	2.3594	2.0878	2.4519
A11; A17	1.0000	2.9817	1.0100	1.3364	1.0293	1.3208	1.2508
A12; A15	1.0000	1.2021	1.4074	1.0548	1.3721	1.2846	1.3155
A13; A16	1.0000	1.2563	2.8499	2.8116	2.0673	2.2003	2.2816
A14	1.0000	3.3276	1.0269	1.1702	1.0000	1.0286	1.0003
Best weight (kg)	336.30	377.20	361.50	362.84	360.8658	359.5543	358.9324
Average weight (kg)	-	381.20	362.04	366.77	364.8521	361.6809	359.0855
Standard deviation	-	4.26	0.52	3.742	2.9650	1.7354	0.1246
No. of FE analyses	-	-	20,000	-	4,000	8,000	8,000

Table 11 The optimal natural frequencies of the 37-bar planar truss obtained by different algorithms

Frequency No.	Initial	PSO [5]	HS [10]	CSS [8]	SOS [17]	This work	
						ACCS	EACCS
1	8.89	20.0001	20.0037	20.0000	20.0366	20.0084	20.0003
2	28.82	40.0003	40.0050	40.0693	40.0007	40.0280	40.0058
3	46.92	60.0001	60.0082	60.6982	60.0138	60.0397	60.0049
4	63.62	73.0440	77.9753	75.7339	-	76.8668	76.4605
5	76.87	89.8240	96.2564	97.6137	-	96.7594	96.6879

Table 12 Comparison of optimal results of the 52-bar dome truss obtained by different algorithms

Design variable Z_j, X_j (m); A_i (cm²)	Initial	GA [22]	PSO [5]	HS [10]	CSS [9]	CBO [25]	This work	
							ACCS	EACCS
Z_A	6.0	5.8851	5.5344	4.7374	5.2716	5.6523	6.0230	6.1496
X_B	2.0	1.7623	2.0885	1.5643	1.5909	1.9665	2.1831	2.2497
Z_B	5.7	4.4091	3.9283	3.7413	3.7039	3.7378	3.8056	3.8670
X_F	4.0	3.4406	4.0255	3.4882	3.5595	3.7620	4.0401	4.1004
Z_F	4.5	3.1874	2.4575	2.6274	2.5757	2.5741	2.5015	2.5002
A_1	2.0	1.0000	0.3696	1.0085	1.0464	1.0009	1.0037	1.0002
A_2	2.0	2.1417	4.1912	1.4999	1.7295	1.3326	1.1422	1.1116
A_3	2.0	1.4858	1.5123	1.3948	1.6507	1.3751	1.3115	1.2031
A_4	2.0	1.4018	1.5620	1.3462	1.5059	1.6327	1.3726	1.2816
A_5	2.0	1.911	1.9154	1.6776	1.7210	1.5521	1.3898	1.3620
A_6	2.0	1.0109	1.1315	1.3704	1.0020	1.0000	1.3883	1.3462
A_7	2.0	1.4693	1.8233	1.4137	1.7415	1.6071	1.3165	1.2910
A_8	2.0	2.1411	1.0904	1.9378	1.2555	1.3354	1.5172	1.6409
Best weight (kg)	338.69	236.046	228.381	214.94	205.237	197.962	199.2701	198.8307
Average weight (kg)	–	–	234.30	229.88	213.101	206.858	206.2003	199.6934
Standard deviation	–	–	5.22	12.44	7.391	5.750	6.5425	1.9257
No. of analyses	–	–	–	20,000	4,000	4,000	8,000	8,000

Table 13 The optimal natural frequencies of the 52-bar dome truss obtained by different algorithms

Frequency No.	Initial	GA [22]	PSO [5]	HS [10]	CSS [9]	CBO [25]	This work	
							ACCS	EACCS
1	22.69	12.81	12.751	12.2222	9.246	10.2404	11.3007	11.7189
2	25.17	28.65	28.649	28.6577	28.648	28.6482	28.6481	28.6477
3	25.17	28.65	28.649	28.6577	28.699	28.6504	28.6538	28.6486
4	31.52	29.54	28.803	28.6618	28.735	28.7117	28.6594	28.6548
5	33.80	30.24	29.230	30.0997	29.223	29.2045	28.7886	28.8702

4.2 Shape and size optimization
4.2.1 The 37-bar planar truss
A simply supported 37-bar planar truss is studied as the shape and size optimization example to demonstrate the effectiveness and robustness of the EACCS. Fig. 10 shows the initial shape and a finite element model of this structure. A constant lumped mass of 10 kg is placed on each free node of the lower chord, and is assumed to be unchanged during the design process. All bars of the lower chord are fixedly assigned to a constant cross-sectional area of 4×10^{-3} m², whereas the others possess an initial cross-sectional area of 1×10^{-4} m². It should be noted that all the nodes of the upper chord are permitted to move vertically, their y-axis coordinates are thus taken as design variables. Furthermore, nodal coordinates and member areas are connected so that the structure is symmetric. Consequently, nineteen design variables containing five nodal coordinate and fourteen cross-sectional areas are redesigned. This structure which is a well-known benchmark problem has been previously studied by many researchers [4, 5, 10, 17, 22, 24–26].
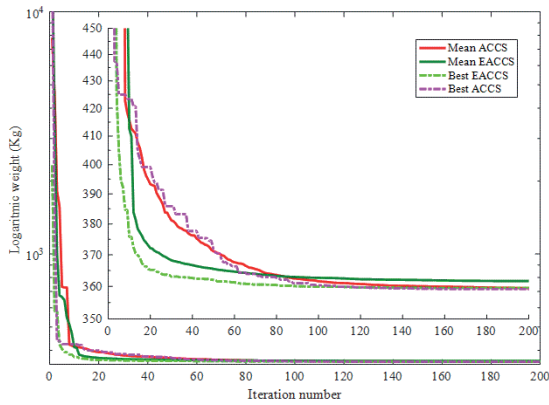
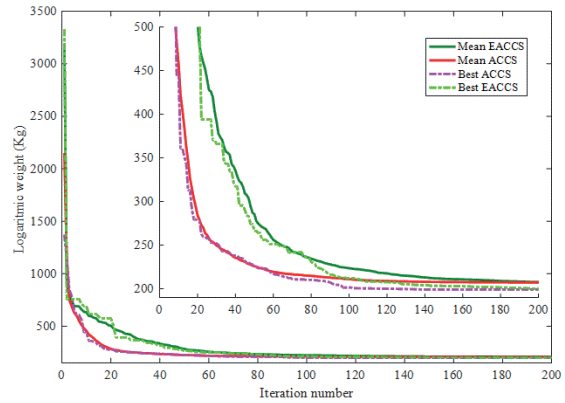**Fig. 12** The weight convergence histories of the 37-bar planar truss obtained using the ACCS and EACCS

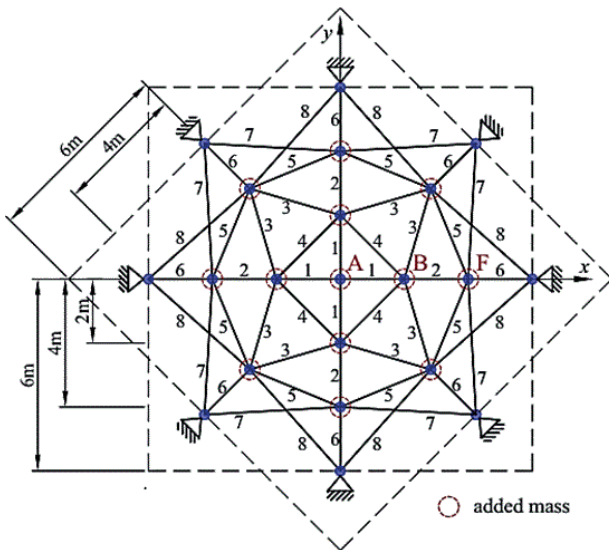**Fig. 15** The weight convergence histories of the 52-bar dome truss
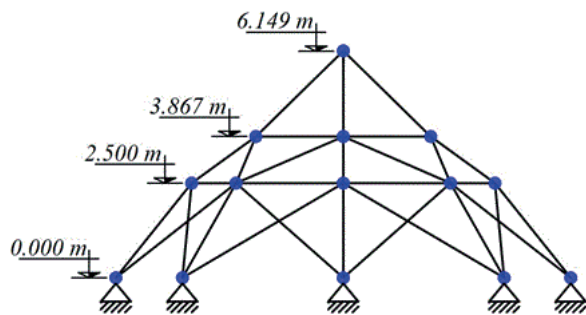
Optimal results obtained by both algorithms and different approaches including cross-sectional areas, nodal coordinates, corresponding weights and statistics results are provided in Table 10. It can be seen that the EACCS results in better solutions than the others.

Table 11 represents the first five optimal natural frequencies attained by the present study and different algorithms. As can be observed, all the optimized frequencies are free from any violations of constraints. Fig. 11 describes the optimal shape of the truss structure obtained using the EACCS. It can be stated that this final shape is quite similar to those obtained in the previously published works. Finally, the convergence rate of the ACCS and EACCS are illustrated in Fig. 12.

4.2.2 The 52-bar dome truss

The last example for the shape and size optimization problem is considered as a 52-bar dome truss. The initial schematic of the structure is depicted in Fig. 13. For optimization purpose, the members of the structure are divided into eight variable groups as labeled in the same figure. With each free node a mass of 50 kg is assigned. The three coordinates (x, y, z) of each free node can shift within the range ±2 m, and these are also considered as design variables. It should be noted that the entire structure must preserve its symmetry during the optimization process. Thus, there are thirteen independent design variables consisting of five shape and eight size variables. All member areas are initially assigned a value of 2×10^{-4} m^2. This dome truss is a well-known benchmark problem has previously been studied by researchers such as [5–10, 17, 24, 27].

Table 12 contains a comparison of the optimal results obtained by both ACCS and EACCS algorithms, and the other considered approaches. The effectiveness and robustness of the EACCS, the optimal weight achieved by

Fig. 13 The initial shape of the 52-bar dome truss

Fig. 14 Final configuration found by the artificial coronary circulation system for the spatial 52-bar truss

the proposed method is the best compared to those given by the other considered algorithms as indicated in the table. Table 13 displays the first five optimal natural frequencies for different optimization methods. It can easily be seen that no violation of constraints are present for the optimized results. Fig. 14 sketches the final optimal shape of the structure given by the EACCS after the design process. It should be noted that similar configurations were also found by various studies in the literature. Fig. 15 shows the weight convergence histories obtained using the EACCS for this structure.

5 Conclusions

In this paper, a new enhanced ACCS is proposed for dealing with shape and size optimization problems of truss structures under multiple frequency constraints. The present algorithm is a bio-inspired population-based meta-heuristic based on the re-growing behavior of the capillaries and arteries, which can happen repeatedly. Six numerical benchmark examples with highly nonlinear and non-convex properties including four examples for size optimization and two examples for shape and size optimization are tested to verify the effectiveness and robustness of the proposed approach.

The results are compared with those of some other optimization algorithms on the same problems. The results indicate that the performance of the EACCS is comparable to the other state-of-the-art methods. In fact, for six of the examples, EACCS found the best results among the compared methods.

Therefore, the EACCS is very promising algorithm to extend its applications to various engineering optimization problems in many fields with the high feasibility where the computational cost is important. Also, the EACCS is a multi-purpose optimization algorithm which can be used for other types of optimization problems from different fields of science and engineering. Application of the EACCS to different classes of optimization problems, and investigation of possible variants and modifications, could be the subject of future studies. Form the results of this study it can be concluded that both standard ACCS and its enhanced version have performed better than the many other methods available in the literature in some of the examples considered, and in one example the design is only slightly heavier than the best one found.

References

[1] Pholdee, N., Bureerat, S. "Comparative performance of meta-heuristic algorithms for mass minimisation of trusses with dynamic constraints", Advances in Engineering Software, 75, pp. 1–13, 2014.
https://doi.org/10.1016/j.advengsoft.2014.04.005

[2] Tejani, G. G., Savsani, V. J., Patel, V. K., Mirjalili, S. "Truss optimization with natural frequency bounds using improved symbiotic organisms search", Knowledge-Based Systems, 143, pp. 162–178, 2018.
https://doi.org/10.1016/j.knosys.2017.12.012

[3] Grandhi, R. V., Venkayya, V. B. "Structural optimization with frequency constraints", AIAA journal, 26(7), pp. 858–866, 1988.
https://doi.org/10.2514/3.9979

[4] Wang, D., Zhang, W. H., Jiang, J. S. "Truss optimization on shape and sizing with frequency constraints", AIAA journal, 42(3), pp. 622–630, 2004.
https://doi.org/10.2514/1.1711

[5] Gomes, H. M. "Truss optimization with dynamic constraints using a particle swarm algorithm", Expert Systems with Applications, 38(1), pp. 957–968, 2011.
https://doi.org/10.1016/j.eswa.2010.07.086

[6] Kaveh, A., Ilchi Ghazaan, M., Bakhshpoori, T. "An improved ray optimization algorithm for design of truss structures", Periodica Polytechnica Civil Engineering, 57(2), pp. 97–112, 2013.
https://doi.org/10.3311/PPci.7166

[7] Kaveh, A., Zolghadr, A. "Democratic PSO for truss layout and size optimization with frequency constraints", Computers & Structures, 130, pp. 10–21, 2014.
https://doi.org/10.1016/j.compstruc.2013.09.002

[8] Kaveh, A., Zolghadr, A. "Truss optimization with natural frequency constraints using a hybridized CSS-BBBC algorithm with trap recognition capability", Computers & Structures, 102–103, pp. 14–27, 2012.
https://doi.org/10.1016/j.compstruc.2012.03.016

[9] Kaveh, A., Zolghadr, A. "Shape and size optimization of truss structures with frequency constraints using enhanced charged system search algorithm", Asian Journal of Civil Engineering, 12(4), pp. 487–509, 2011. [online] Available at: https://www.sid.ir/en/journal/ViewPaper.aspx?id=248035 [Accessed: 23 January 2019]

[10] Miguel, L. F. F., Miguel, L. F. F. "Shape and size optimization of truss structures considering dynamic constraints through modern metaheuristic algorithms", Expert Systems with Applications, 39(10), pp. 9458–9467, 2012.
https://doi.org/10.1016/j.eswa.2012.02.113

[11] Savsani, V. J., Tejani, G. G., Patel, V. K. "Truss topology optimization with static and dynamic constraints using modified sub-population teaching–learning-based optimization", Engineering Optimization, 48(11), pp. 1990–2006, 2016.
https://doi.org/10.1080/0305215X.2016.1150468

[12] Kaveh, A., Mahdavi, V. R. "Optimal design of structures with multiple natural frequency constraints using a hybridized BB-BC/Quasi-Newton algorithm", Periodica Polytechnica Civil Engineering, 57(1), pp. 27–38, 2013.
https://doi.org/10.3311/PPci.2139

[13] Kaveh, A., Ilchi Ghazaan, M. "Vibrating particles system algorithm for truss optimization with multiple natural frequency constraints", Acta Mechanica, 228(1), pp. 307–322, 2017.
https://doi.org/10.1007/s00707-016-1725-z

[14] Kaveh, A., Ilchi Ghazaan, M. "Enhanced colliding bodies algorithm for truss optimization with frequency constraints", Journal of Computing in Civil Engineering, 29(6), 2015.
https://doi.org/10.1061/(ASCE)CP.1943-5487.0000445

[15] Kaveh, A., Zolghadr, A. "Topology optimization of trusses considering static and dynamic constraints using the CSS", Applied Soft Computing, 13(5), pp. 2727–2734, 2013.
https://doi.org/10.1016/j.asoc.2012.11.014

[16] Savsani, V. J., Tejani, G. G., Patel, V. K., Savsani, P. "Modified meta-heuristics using random mutation for truss topology optimization with static and dynamic constraints", Journal of Computational Design and Engineering, 4(2), pp. 106–130, 2017.
https://doi.org/10.1016/j.jcde.2016.10.002

[17] Tejani, G. G., Savsani, V. J., Patel, V. K. "Adaptive symbiotic organisms search (SOS) algorithm for structural design optimization", Journal of Computational Design and Engineering, 3(3), pp. 226–249, 2016.
https://doi.org/10.1016/j.jcde.2016.02.003

[18] Maute, K., Frangopol, D. M. "Reliability-based design of MEMS mechanisms by topology optimization", Computers & Structures, 81(8–11), pp. 813–824, 2003.
https://doi.org/10.1016/S0045-7949(03)00008-7

[19] Yildiz, A. R. "A new hybrid particle swarm optimization approach for structural design optimization in the automotive industry", Proceedings of the Institution of Mechanical Engineers, Part D: Journal of Automobile Engineering, 226(10), pp. 1340–1351, 2012.
https://doi.org/10.1177%2F0954407012443636

[20] Yildiz, A. R. "Comparison of evolutionary-based optimization algorithms for structural design optimization", Engineering Applications of Artificial Intelligence, 26(1), pp. 327–333, 2013.
https://doi.org/10.1016/j.engappai.2012.05.014

[21] Kooshkbaghi, M., Kaveh, A. "Sizing optimization of truss structures with continuous variables by artificial coronary circulation system algorithm", Iranian Journal of Science and Technology, in press, 2019.

[22] Lingyun, W., Mei, Z., Guangming, W., Guang, M. "Truss optimization on shape and sizing with frequency constraints based on genetic algorithm", Computational Mechanics, 35(5), pp. 361–368, 2005.
https://doi.org/10.1007/s00466-004-0623-8

[23] Zuo, W., Xu, T., Zhang, H., Xu, T. "Fast structural optimization with frequency constraints by genetic algorithm using adaptive eigenvalue reanalysis methods", Structural and Multidisciplinary Optimization, 43(6), pp. 799–810, 2011.
https://doi.org/10.1007/s00158-010-0610-y

[24] Wei, L., Tang, T., Xie, X., Shen, W. "Truss optimization on shape and sizing with frequency constraints based on parallel genetic algorithm", Structural and Multidisciplinary Optimization, 43(5), pp. 665–682, 2011.
https://doi.org/10.1007/s00158-010-0600-0

[25] Kaveh, A., Mahdavi, V. R. "Colliding bodies optimization method for optimum design of truss structures with continuous variables", Advances in Engineering Software, 70, pp. 1–12, 2014.
https://doi.org/10.1016/j.advengsoft.2014.01.002

[26] Kaveh, A., Mahdavi, V. R. "Colliding-bodies optimization for truss optimization with multiple frequency constraints", Journal of Computing in Civil Engineering, 29(5), 2015.
https://doi.org/10.1061/(ASCE)CP.1943-5487.0000402

[27] Lin, J. H., Che, W. Y., Yu, Y. S. "Structural optimization on geometrical configuration and element sizing with statical and dynamical constraints", Computers & Structures, 15(5), pp. 507–515, 1982.
https://doi.org/10.1016/0045-7949(82)90002-5

[28] Farshchin, M., Camp, C. V., Maniat, M. "Multi-class teaching–learning-based optimization for truss design with frequency constraints", Engineering Structures, 106, pp. 355–369, 2016.
https://doi.org/10.1016/j.engstruct.2015.10.039